Multimagnon bound states in an easy-axis frustrated ferromagnetic spin chain

D. V. Dmitriev* and V. Ya. Krivnov
Joint Institute of Chemical Physics of RAS, Kosygin Str. 4, 119334 Moscow, Russia
(Received 9 December 2008; revised manuscript received 13 January 2009; published 18 February 2009)

The frustrated spin-1/2 chain with weakly anisotropic ferromagnetic nearest-neighbor and antiferromagnetic next-nearest-neighbor exchanges is studied using the scaling estimates of the perturbation theory and numerical calculations. We focus on the excitation spectrum and the low-temperature thermodynamics in the ferromagnetic region of the ground-state phase diagram. It is shown that the excitation spectrum of the model is characterized by the existence of the multimagnon bound states. These excitations determine the low-temperature magnetic susceptibility. The energy of the bound magnon complexes is found and the relation of the considered model to the edge-sharing cuprate Li_2CuO_2 is discussed.

DOI: 10.1103/PhysRevB.79.054421 PACS number(s): 75.10.Jm, 75.10.Pq

I. INTRODUCTION

The quantum spin chains with nearest-neighbor (NN) J_1 and next-nearest-neighbor (NNN) interactions J_2 have been a subject of numerous studies.[1] The model with both antiferromagnetic (AF) interactions J_1, $J_2>0$ (AF-AF model) is well studied.[2–7] Lately, there has been considerable interest in the study of ferromagnetic (F)-AF model with the ferromagnetic NN and the antiferromagnetic NNN interactions $(J_1<0, J_2>0)$.[8–13] One of the reasons is understanding of intriguing magnetic properties of a novel class of quasi-one-dimensional edge-sharing copper oxides, which are described by the F-AF model.[14–19]

The Hamiltonian of the spin-1/2 F-AF model is

$$H = J_1 \sum_{n=1}^{N} (S_n^x S_{n+1}^x + S_n^y S_{n+1}^y + \Delta_1 S_n^z S_{n+1}^z) + J_2 \sum_{n=1}^{N} (S_n^x S_{n+2}^x + S_n^y S_{n+2}^y + \Delta_2 S_n^z S_{n+2}^z), \quad (1)$$

where $J_1<0$ and $J_2>0$. The isotropic case of this model $(\Delta_1=\Delta_2=1)$ is intensively studied in the past years.[11,12,20–22] The model with the anisotropy of exchange interactions is less studied. Though the anisotropy in real chain is weak,[23] it influences on the properties of such compounds. The ground-state phase diagram of model (1) with small anisotropy has been studied by us in Ref. 24. As shown in Fig. 1, the phase diagram consists of three phases: commensurate spin-liquid gapless phase, the incommensurate phase with spin correlations of a spiral type, and fully polarized ferromagnetic phase. Though this phase diagram is related to the particular case of the anisotropic NN and isotropic NNN interactions, model (1) with both $\Delta_1 \neq 1$ and $\Delta_2 \neq 1$ has the phase diagram qualitatively similar to that shown in Fig. 1.[24] The point $|J_2/J_1|=1/4$ is the transition point for the isotropic model $(\Delta_1=\Delta_2=1)$, where the transition from the ferromagnetic to the incommensurate ground state with $S^z=0$ occurs. This transition is the second-order one. For the anisotropic model the phase transition between the ferromagnetic and the incommensurate states is of the first-order type.

The properties of the commensurate spin-fluid and the incommensurate phases have been studied in Ref. 24. In this paper we study the properties of the F phase. Though the ferromagnetic ground state is very simple, the excitation spectrum is not trivial. The important feature of the spectrum is the existence of two types of excitations: conventional spin waves and the multimagnon bound states. These excitations govern the low-temperature thermodynamics of the model in the F phase. The additional motivation of the study of this phase is the fact that the ferromagnetic in-chain ordering has been observed in some edge-sharing cuprates.[25] This indicates that the frustration parameter $\lambda \equiv |J_2/J_1|$ can be less than 1/4 in these compounds.[26]

For simplicity we confine our study to the case of the anisotropy of the NN interaction only, i.e., we consider Hamiltonian (1) with $\Delta_1=\Delta>1$ and $\Delta_2=1$,

$$H = -\sum \left(S_n^x S_{n+1}^x + S_n^y S_{n+1}^y + \Delta S_n^z S_{n+1}^z - \frac{\Delta}{4} \right) + \lambda \sum \left(\mathbf{S}_n \cdot \mathbf{S}_{n+2} - \frac{1}{4} \right), \quad (2)$$

where we take $|J_1|$ as an energy unit and add constant shifts to secure the energy of the fully polarized state to be zero. In our study we will pay a special attention to the vicinity of the

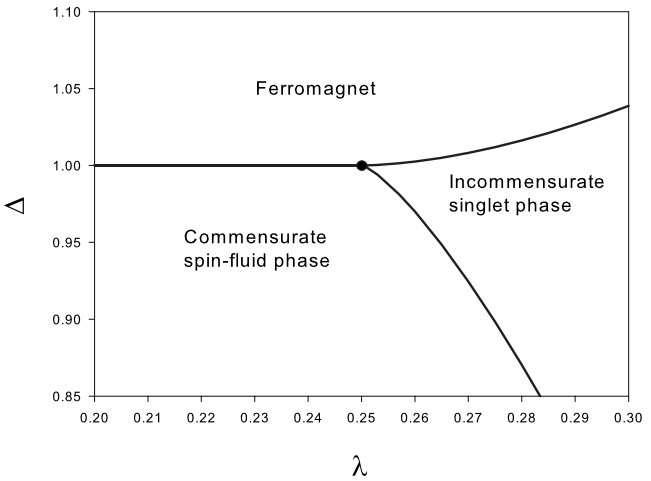

FIG. 1. The phase diagram of model (2) (Ref. 24).

transition point ($\lambda=1/4, \Delta=1$), where the spectrum of model (2) sharply changes.

The paper is organized as follows. In Sec. II we represent the known results for model (2) at $\lambda=0$. In Sec. III we exactly calculate the two-magnon bound energy. In Sec. IV we perform the scaling estimates for the energy of the multimagnon bound states based on the analysis of infrared divergencies in the perturbation theory (PT) in small parameter $\alpha \equiv \Delta-1$. In Sec. V we present results of numerical calculations of finite chains. In Sec. VI we study the low-temperature thermodynamics of model (2) and determine the region of parameters where the multimagnon excitations dominate. The relevance of the F-AF anisotropic model to the copper oxide Li_2CuO_2 is discussed in Sec. VII.

II. BOUND STATES IN THE FERROMAGNETIC CHAIN

In this section we review the known results relevant to our study. In the special case $\lambda=0$ model (2) reduces to the ferromagnetic *XXZ* chain with the Ising-type anisotropy. Its ground state is ferromagnetic with zero energy and with the gap in the excitation spectrum. Lowest-lying excitations are bound states of overturned spins from the fully polarized ground state (multimagnon bound states). The energy of m-magnon bound state $E_m(k)$ for the chain with the periodic boundary conditions (ring) was found by Ovchinnikov[27] using the Bethe ansatz. He showed that $E_m(k)$ at $N\to\infty$ is

$$E_m(k)=\frac{\sinh(\nu)[\cosh(m\nu)-\cos k]}{\sinh(m\nu)}, \tag{3}$$

where k is a total momentum, $\cosh\nu=\Delta$, and $m=1,2,\ldots$.

For $k=0$ the above equation reduces to

$$E_m \equiv E_m(0)=\sinh(\nu)\tanh\left(\frac{m\nu}{2}\right). \tag{4}$$

In particular, for one- and two-magnon states it gives

$$E_1=\Delta-1,$$

$$E_2=\Delta-\frac{1}{\Delta} \tag{5}$$

(certainly, there is no bound state for $m=1$; in this case Eq. (3) describes the one-magnon spectrum). It follows from Eq. (3) that the energy of the m-magnon bound state saturates exponentially with m to the value $E_s=\sqrt{\Delta^2-1}$ and does not depend on k for $m\gg 1$, i.e., excitations become dispersionless.

Another important result for model (2) at $\lambda=0$ was obtained by Alcaraz *et al.* in Ref. 28, where the multimagnon bound states were studied for the chain with free-end boundary conditions (open chains). The Bethe ansatz solution gives the energy of the m-magnon bound state in the open chain in a form[28]

$$E_{m,\text{open}}=\sum_{i=1}^{m}\left[\Delta-\frac{1}{2}\left(\rho_i-\frac{1}{\rho_i}\right)\right], \tag{6}$$

where ρ_i is defined by a recurrence equation,

$$\rho_{i+1}=\frac{1}{2\Delta-\rho_i} \tag{7}$$

with $\rho_1=1/\Delta$.

We found that the solution of Eq. (7) gives for $E_{m,\text{open}}$,

$$E_{m,\text{open}}=\frac{1}{2}\sqrt{\Delta^2-1}\,\tanh(m\nu). \tag{8}$$

The comparison of Eq. (8) with Eq. (4) leads to the exact relation,

$$E_{2m}=2E_{m,\text{open}}. \tag{9}$$

This relation means that the energy of the multimagnon bound state in the open chain at $m\gg 1$ saturates to a value which is a half of that for the ring. This property has been observed earlier[29] in numerical calculations of model (2) for $\lambda=0$. Actually, the validation of Eq. (9) looks quite natural because it implies that the magnetic soliton of size $2m$ can be represented as two kinks of size m.

As was shown in Ref. 29 a low-temperature thermodynamics of the anisotropic ferromagnetic chain is determined by an effective gap which is the lowest of two values: the gap for the one-magnon excitations E_1 (spin waves) and the gap for the multimagnon bound states for the *open* chain (not ring) $E_{m,\text{open}}$. The comparison of Eqs. (5) and (8) shows that the effective gap for $\Delta<5/3$ is the spin-wave gap $E_1=\Delta-1$, while for $\Delta>5/3$ it is the multimagnon bound-state energy equal to $E_{\text{kink}}=\frac{1}{2}\sqrt{\Delta^2-1}$. As will be shown below, many peculiarities of the excitation spectrum of the anisotropic ferromagnet remain for model (2) with $\lambda\neq 0$.

III. ONE- AND TWO-MAGNON EXCITATIONS

In this section we consider the one- and two-magnon states for frustrated model (2) with $\lambda\neq 0$. We begin with the case of the rings with periodic boundary conditions. The energy of the one-magnon state is

$$E_1(k)=\Delta-\cos k-\lambda[1-\cos(2k)]. \tag{10}$$

The one-magnon spectrum has a minimum at $k=0$ for $0\le\lambda\le 1/4$ and has a double-well form with two minima at $k=\pm\arccos[1/(4\lambda)]$ for $\lambda>1/4$. The expansion of $E_1(k)$ at small k ($\alpha\equiv\Delta-1$),

$$E_1(k)=\alpha+\frac{1-4\lambda}{2}k^2+\frac{16\lambda-1}{24}k^4+\cdots, \tag{11}$$

shows that the behavior of the low-lying excitations on the isotropic line $\Delta=1$ is different: in the region $0\le\lambda<1/4$ the low-lying excitations are described by k^2 spectrum,

$$E_1(k)=\frac{1-4\lambda}{2}k^2, \quad \lambda<1/4, \tag{12}$$

while at the transition point $\lambda=1/4$ the one-magnon spectrum becomes

$$E_1(k) = \frac{k^4}{8}, \quad \lambda = 1/4. \tag{13}$$

As was shown in Ref. 24 this difference plays a key role in the change in the critical exponents near the transition point $\lambda = 1/4$.

A remarkable feature of the two-magnon spectrum is the existence of the bound states lying below the scattering continuum. For the isotropic F-AF model ($\Delta = 1$) the two-magnon bound states at $\lambda > 1/4$ have been studied in detail earlier.[9,20,21,30–32] In particular, it was shown that, namely, these states define the saturation magnetic field in the incommensurate phase for $\lambda \gtrsim 0.367$.[33]

Fortunately, the two-magnon bound-state energy $E_2(k)$ can be found exactly for general anisotropic case of model (2). The analysis of the scattering problem of two magnons shows that for each total momentum k of the magnon pair there is one bound state. The minimization of the energy $E_2(k)$ over k gives the gap in the two-magnon spectrum. In general, the dependence of $k_{\min}(\Delta, \lambda)$ minimizing $E_2(k)$ is rather complicated. We note only that $k_{\min} \to \pi$ when Δ is increased at fixed λ and the dependence of the value $\Delta_\pi(\lambda)$ was found in Ref. 30.

We are interested mainly in two-magnon bound states in the ferromagnetic phase in the vicinity of the transition point $\lambda = 1/4$ and for weak anisotropy $\alpha \ll 1$. In this region the energy $E_2(k)$ has a minimum at $k = 0$. Therefore, hereinafter we restrict ourselves to the two-magnon excitations with $k = 0$. For this case the standard method of calculation of two-magnon states[34] is simplified and the two-magnon bound-state energy E_2 is determined from the equation

$$\frac{1}{\pi}\int_0^\pi \frac{E_1(q)dq}{E_2 - 2E_1(q)} = -1, \tag{14}$$

where $E_1(q)$ is the spectrum of the one-magnon excitations given by Eq. (10).

Evaluating the integral in Eq. (14) we obtain the following algebraic equation for E_2:

$$[(2\Delta - E_2)^2 - 4][1 - 2\lambda(2\Delta - E_2) + 2\lambda\sqrt{(2\Delta - E_2)^2 - 4}] = E_2^2. \tag{15}$$

For $\lambda = 0$ the solution of this equation reproduces the exact result [Eq. (5)]. Let us represent E_2 in the form

$$E_2 = 2\alpha - \frac{\gamma^2}{4\lambda}\Theta(-\gamma) - E_b, \tag{16}$$

where Θ is the Heaviside function, $\gamma = 1 - 4\lambda$, and E_b is the binding energy relative to the two-magnon scattering continuum.

The series expansion of the binding energy in small parameter α for $\lambda < 1/4$ is

$$E_b = \frac{\alpha^2}{\gamma} - \frac{\alpha^3}{\gamma^{5/2}}(1 + \gamma^{1/2} - \gamma) + O(\alpha^4). \tag{17}$$

At the transition point $\lambda = 1/4$ the solution of Eq. (15) gives

$$E_b = \alpha^{4/3} - \frac{2}{3}\alpha^{5/3} + O(\alpha^2). \tag{18}$$

Near the transition point ($\alpha \ll 1, |\gamma| \ll 1$) Eq. (15) can be simplified to the cubic equation,

$$[E_b + \gamma^2\Theta(-\gamma)]^{3/2} + \gamma[E_b + \gamma^2\Theta(-\gamma)] = \alpha^2. \tag{19}$$

The solution of Eq. (19) has a scaling form depending on a scaling variable $\kappa = \gamma/\alpha^{2/3}$,

$$E_b = \alpha^{4/3} g(\kappa), \tag{20}$$

where the function $g(\kappa)$ is a solution of equation

$$[g + \kappa^2\Theta(-\kappa)]^{3/2} + \kappa[g + \kappa^2\Theta(-\kappa)] = 1. \tag{21}$$

In the limits $\kappa \to \infty (\gamma \gg \alpha^{2/3})$ the asymptotic of $g(\kappa)$ reproduces the leading terms of Eq. (17). In the region close to the line $\lambda = 1/4$, when $|\gamma| \ll \alpha^{2/3}$ ($|\kappa| \ll 1$) the expansion of $g(\kappa) = 1 - 2\kappa/3 + \cdots$ results in the following series for the binding energy,

$$E_b = \alpha^{4/3} - \frac{2}{3}\gamma\alpha^{2/3} + O(\gamma^2), \tag{22}$$

which contains the corrections to the leading term in Eq. (18).

In the region $\lambda \gtrsim \frac{1}{4}$ the binding energy vanishes on the curve $2\alpha = \gamma^2$. Near this curve according to Eq. (15) the binding energy behaves as

$$E_b = \frac{(2\alpha - \gamma^2)^2}{2|\gamma|}. \tag{23}$$

Thus, the critical exponent characterizing a power-law dependence of the binding energy on α changes from 2 at $\lambda = 0$ to 4/3 at $\lambda = 1/4$. This change is due to the modification of the behavior of the one-magnon energy at small k [Eqs. (12) and (13)].

For further study it is useful to estimate the finite-size corrections to the two-magnon binding energy. For finite rings the integral in Eq. (14) is replaced by a sum,

$$\frac{1}{N}\sum_k \frac{E_1(k)}{E_2 - 2E_1(k)} = -1 \tag{24}$$

with $k = \frac{2\pi n}{N}$ and $n = -N/2, \ldots, N/2$. The calculation of this sum gives the finite-size correction for the leading term of the binding energy

$$E_b = \frac{\alpha^2}{\gamma}(1 + 4e^{-N\alpha/\gamma}) \tag{25}$$

for $\lambda < 1/4$ and

$$E_b = \alpha^{4/3}\left[1 - \frac{8\sqrt{2}}{3}e^{-N\alpha^{1/3}}\sin\left(N\alpha^{1/3} + \frac{\pi}{4}\right)\right] \tag{26}$$

for $\lambda = 1/4$.

Thus, we found the exponentially small finite-size effects, which is not a surprise for the bound states. More important is that we identified the scaling parameters $N\alpha/\gamma$ for $\lambda < 1/4$ and $N\alpha^{1/3}$ for $\lambda = 1/4$, which will be exploited later.

At the end of this section it is worthwhile to make a following remark. Let us consider the one-magnon states in the open chains. The one-magnon problem in this case can be solved by a standard method. The spectrum of the one-magnon excitations consists of $(N-2)$ band states, the energies of which coincide at $N\to\infty$ with those given by Eq. (10). However, there are two degenerated bound states localized near chain ends. Remarkably, the energy $E_{1,\mathrm{open}}$ of these bound states is determined by Eq. (15) with the substitution of $2E_{1,\mathrm{open}}$ for E_2. Thus, the energy of the one-magnon bound states in the open chain is half of the energy of the two-magnon bound state with $k=0$ in the ring. It means that relation (9) remains valid for the case $m=1$.

IV. PERTURBATION THEORY

For more than two magnons the exact analytic solution is not possible excluding the case $\lambda=0$. Therefore, for studying the multimagnon bound states we develop the PT in small parameter α. At first, we inspect how the energy of the two-magnon state obtained in Sec. III can be estimated in the framework of the PT.

A. Perturbation theory for two-magnon states

Let us represent Hamiltonian (2) in a form

$$H = H_1 + \lambda V_2 + \alpha V_z,$$

$$H_1 = -\sum\left(\mathbf{S}_n\cdot\mathbf{S}_{n+1} - \frac{1}{4}\right),$$

$$V_2 = \sum\left(\mathbf{S}_n\cdot\mathbf{S}_{n+2} - \frac{1}{4}\right),$$

$$V_z = -\sum\left(S_n^z S_{n+1}^z - \frac{1}{4}\right). \tag{27}$$

We use the perturbation theory in small parameter α, so that a small perturbation αV_z is added to the unperturbed Hamiltonian $H_0=H_1+\lambda V_2$. The ground state of H_0 for $\lambda\le 1/4$ is ferromagnetic (total spin $S=N/2$) and is degenerate with respect to total S^z. The perturbation αV_z splits this degeneracy. We consider the two-magnon sector; therefore, we develop the PT to the ferromagnetic state with the projection $S^z=N/2-2$, which we denote as $|\psi_0\rangle$.

In the first order of PT we have

$$E^{(1)} = \langle\psi_0|\alpha V_z|\psi_0\rangle = 2\alpha. \tag{28}$$

So the second and all higher orders of the PT define the two-magnon binding energy [Eq. (16)],

$$E_b(\alpha) = -\langle\psi_0|\alpha^2 V_z\frac{1}{E_0-H_0}V_z + \alpha^3 V_z\frac{1}{E_0-H_0}V_z\frac{1}{E_0-H_0}V_z + \cdots|\psi_0\rangle. \tag{29}$$

Suppose that the main contributions to the binding energy are given by the low-lying excitations. Then the higher orders of the perturbation series contain more dangerous denominators and, therefore, possibly have higher powers of the infrared divergency. Therefore, we use scaling arguments to estimate the critical exponent for the binding energy. Below we will pay attention only to the powers of the divergent terms and omit numerical factors.

Collecting the most divergent parts in all orders of the PT, we express the correction to the binding energy as[35]

$$E_b = \langle\psi_q|\alpha V_z|\psi_{q'}\rangle f(x), \tag{30}$$

where $|\psi_q\rangle$ are two-magnon states involved into the PT and $f(x)$ is a scaling function of a scaling parameter,

$$x \sim \frac{\langle\psi_q|\alpha V_z|\psi_{q'}\rangle}{E_q - E_0}, \tag{31}$$

which absorbs the infrared divergencies.

The state $|\psi_0\rangle$ has the total momentum $k=0$. The perturbation V_z preserves the total momentum k and the projection S^z. Therefore, only two-magnon states $|\psi_q\rangle$ with $k=0$ are involved into the PT. The analysis shows that the matrix elements of the perturbation operator V_z between the states $|\psi_q\rangle$ involved in the PT behave as

$$\langle\psi_q|V_z|\psi_{q'}\rangle \sim 1/N. \tag{32}$$

The N behavior of denominators in Eq. (29) depends on the value of λ. As follows from the one-magnon spectrum [Eqs. (12) and (13)] the denominators behave as

$$E_q - E_0 \sim \gamma N^{-2}, \quad \lambda < 1/4,$$

$$E_q - E_0 \sim N^{-4}, \quad \lambda = 1/4. \tag{33}$$

The estimate of scaling parameter using Eqs. (32) and (33) gives

$$x = \frac{\alpha N}{\gamma}, \quad \lambda < 1/4,$$

$$x = \alpha N^3, \quad \lambda = 1/4. \tag{34}$$

We note that exactly the same scaling parameters were determined in Sec. III [Eqs. (25) and (26)].

In the thermodynamic limit the binding energy tends to a finite value (independent of N). This requires the asymptotic at $x\to\infty$ of the scaling function $f(x)\sim x$ for $\lambda<1/4$ and $f(x)\sim x^{1/3}$ for $\lambda=1/4$. This gives for E_b,

$$E_b \sim \frac{\alpha^2}{\gamma}, \quad \lambda < 1/4,$$

$$E_b \sim \alpha^{4/3}, \quad \lambda = 1/4. \tag{35}$$

The obtained results totally agree with those obtained in Sec. III. Thus, the scaling estimates of divergencies in the PT correctly reproduce the scaling parameters and the leading terms in the energy.

B. Perturbation theory for m-magnon states

We start to study the multimagnon problem from the exactly solvable case $\lambda=0$. The lowest m-magnon energies in

the thermodynamic limit are given by Eq. (4). For small anisotropy $\alpha \ll 1$ the energy E_m can be written as a function of a scaling parameter αm^2,

$$E_m(\alpha) = m\alpha f_0(\alpha m^2) \tag{36}$$

with

$$f_0(x) = \sqrt{\frac{2}{x}}\tanh\left(\sqrt{\frac{x}{2}}\right). \tag{37}$$

For large magnon complexes the parameter $\alpha m^2 \gg 1$ and the energy converge to

$$E_s(\alpha) = \sqrt{2\alpha}. \tag{38}$$

From the solution of two-magnon problem we know that for $m=2$ but finite N, the energy depends on the scaling parameter $x=\alpha N$ [Eq. (34)]. However, for $m>2$ this scaling parameter is modified and becomes $x=\alpha mN$. Thus, for the case when both m and N are large but finite the energy has a scaling form of two scaling parameters,

$$E_m(\alpha) = m\alpha f_1(\alpha m^2, \alpha mN) \tag{39}$$

with $f_1(\alpha m^2, \alpha mN) \to f_0(\alpha m^2)$ at $N \to \infty$.

Now let us consider the case $\lambda \ll 1$. In this case PT (27) contains two small parameters α and λ and, consequently, two channels V_z and V_2. Each channel can produce infrared divergencies and is described by its own scaling parameter.[35] The matrix elements of the operator V_2 at $\lambda \ll 1$ were found in Ref. 24,

$$\langle \psi_i | V_2 | \psi_j \rangle \sim N^{-2}. \tag{40}$$

Such behavior of the matrix elements means that the perturbation V_2 does not produce infrared divergencies and, therefore, does not form the scaling parameter.[24] It is natural to expect that the behavior of the matrix elements of type (40) remains the same up to the point $\lambda = 1/4$. This assumption results in the following expression for the lowest energy in the sectors with small value of S^z ($\alpha m^2 \gg 1$) in the region $0 \le \lambda < 1/4$:

$$E_s(\alpha, \lambda) = A(\lambda)\sqrt{\alpha}, \tag{41}$$

where $A(\lambda)$ is a smooth function with $A(0) = \sqrt{2}$ [see Eq. (38)]. In the vicinity of the transition point the PT contains two perturbations αV_z and $\frac{\gamma}{4} V_2$,

$$H = H_1 + \frac{1}{4}V_2 + \alpha V_z - \frac{\gamma}{4}V_2. \tag{42}$$

In order to make the scaling estimates of the PT in α one needs to know the matrix elements of the operators V_z and V_2. Unfortunately, it is very difficult problem. However, we can assume that the behavior of matrix elements with m and N near the transition point remains the same as for the case $\lambda = 0$. Then, the only difference between these two cases is the modification of the spectrum presenting in denominators in Eq. (31). According to Eq. (33) for the case $\lambda = 1/4$ both scaling parameters of operator V_z in Eq. (39) acquire additional factor N^2 and become $x = \alpha mN^3$ and $y = \alpha m^2 N^2$. The perturbation $\frac{\gamma}{4} V_2$ near the transition point according to Eqs. (31) and (40) produces the scaling parameter $z = \gamma N^2$.[24] Thus, near the transition point the m-magnon energy can be written in a scaling form

$$E_m(\alpha, \gamma) = m\alpha f_{xyz}(x, y, z). \tag{43}$$

In the thermodynamic limit, when all parameters x, y, $z \to \infty$, the scaling function $f_{xyz}(x, y, z)$ becomes a function of two variables μ and ν (independent of N),

$$\mu = \frac{z\sqrt{y}}{x} = \frac{\gamma}{\sqrt{\alpha}},$$

$$\nu = \frac{y^3}{x^2} = \alpha m^4. \tag{44}$$

It is worth noting that the scaling parameter κ obtained in the exact solution of two-magnon problem near the transition point [Eq. (20)] transforms to the parameter μ [Eq. (44)] with increase in m. The m-magnon energy in the thermodynamic limit takes a form

$$E_m(\alpha, \gamma) = m\alpha f_{\mu\nu}(\mu, \nu). \tag{45}$$

For the lowest states in sectors with small value of S^z ($m \sim N/2$), the scaling parameter $\nu \gg 1$ and the multimagnon energy saturates to

$$E_s(\alpha, \gamma) = \alpha^{3/4} f_\mu(\mu). \tag{46}$$

The function $f_\mu(\mu)$ is generally unknown and will be found numerically in Sec. V. However we can determine analytically its behavior in the limit $\mu \to \infty$ when Eq. (46) must reduce to Eq. (41). This requires the asymptotic $f_\mu(\mu) \sim \sqrt{\mu}$ at $\mu \to \infty$ and the energy

$$E_s(\alpha, \gamma) \sim \sqrt{\gamma\alpha}, \quad \alpha < \gamma^2. \tag{47}$$

This in turn means that the function $A(\lambda)$ in Eq. (41) behaves at $\lambda \to 1/4$ as

$$A(\lambda) \sim \sqrt{1 - 4\lambda}. \tag{48}$$

V. NUMERICAL CALCULATIONS

We have carried out exact diagonalizations of finite rings and open chains up to 24 sites. We observed that the multimagnon bound states are formed and the size of domain walls of multimagnon complexes is less than the system size when the corresponding finite-size scaling parameters become large. This imposes natural restrictions on our calculations: $\alpha \gg 1/N^2$ for $\lambda < 1/4$ and $\alpha \gg 1/N^4$ near the transition point. We found that in all such cases the multimagnon bound energies have exponentially small finite-size corrections (for two-magnon binding energy this fact was established analytically in Sec. III). Therefore, we used a linear extrapolation in $\exp(-aN)$ with a fitting parameter a. To check the numerical accuracy of the extrapolation we compared the extrapolated energy for the total $S^z = 0 (m = N/2)$ and $\lambda = 0$ with Eqs. (4) and (8) and found perfect consistency with the exact results. Near the transition point we found that the use of finite chains with $N \le 24$ is sufficient for

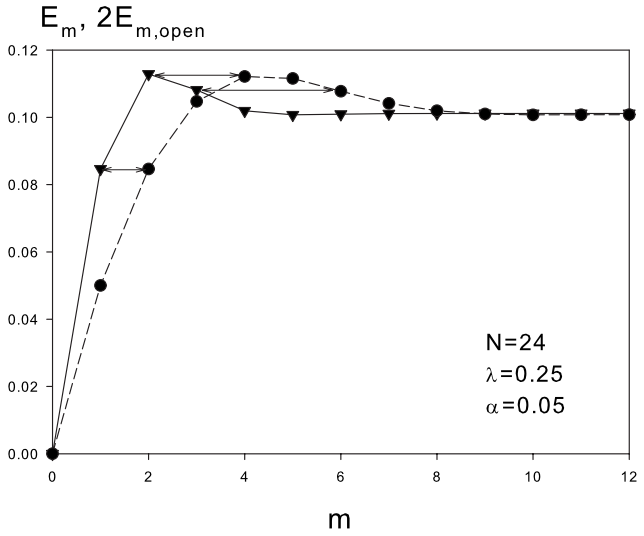

FIG. 2. Energies of the m-magnon bound states of model (2) for rings (circles) and open chains (triangles). Arrows connect a few pairs of points corresponding to double m-magnon energy for open chain $2E_{m,\mathrm{open}}$ and $2m$-magnon energy for ring E_{2m}, validating Eq. (9).

$\alpha \gtrsim 0.001$. We note also that the saturation of the energy E_m at $m \to N/2$ and the convergence to the thermodynamic limit for the open chains occur noticeably faster in comparison with the rings. Really, the kink excitation on open chain of length N corresponds to the soliton excitation on ring of length $2N$. So, the use of open chains effectively doubles the system size and in our numerical calculations we used mostly the open chains in the subspace $S^z=0$.

First, we validated the important relation (9). In Sec. II we have shown that for $\lambda=0$ and $k=0$ the energy of the $2m$-magnon bound state on the ring is double of that for the m-magnon bound state on the open chain. We showed also that at $N \to \infty$ relation (9) is valid for $m=1$ and $\lambda \neq 0$. Unfortunately, we cannot rigorously prove this relation in the general case when $m>1$ and $\lambda \neq 0$ because the analytic solution is not possible in this case. However, we checked numerically that the relative difference $(2E_{m,\mathrm{open}}-E_{2m})/E_{2m}$ vanishes rapidly with N, so that for $N=24$ this difference is less than 0.1% for $m=1,\ldots,6$ in a wide range of values of α and $\lambda \leq 1/4$. Therefore, we suggest that at $N \to \infty$ the energies $2E_{m,\mathrm{open}}$ and E_{2m} do coincide. The typical dependence of the bound-state energy on m for rings and open chains of length $N=24$ is demonstrated in Fig. 2. As follows from Fig. 2 both energies $2E_{m,\mathrm{open}}$ and E_m saturate to the same finite value when $m \gg 1$. Hence, we expect that in the thermodynamic limit and for $m \sim N/2$ the energy of the magnetic soliton doubles the kink energy,

$$E_s(\alpha,\lambda) = 2E_{\mathrm{kink}}(\alpha,\lambda). \tag{49}$$

In Fig. 3 we demonstrate the dependence of the extrapolated lowest energy $E_{\mathrm{kink}}(\alpha)$ in the sector with $S^z=0$ for $\lambda=1/4$. A linear fit of $E_{\mathrm{kink}}/\alpha^{3/4}$ as a function of $\alpha^{1/4}$ gives the equation

$$E_{\mathrm{kink}} \simeq 0.35\alpha^{3/4} + 0.275\alpha. \tag{50}$$

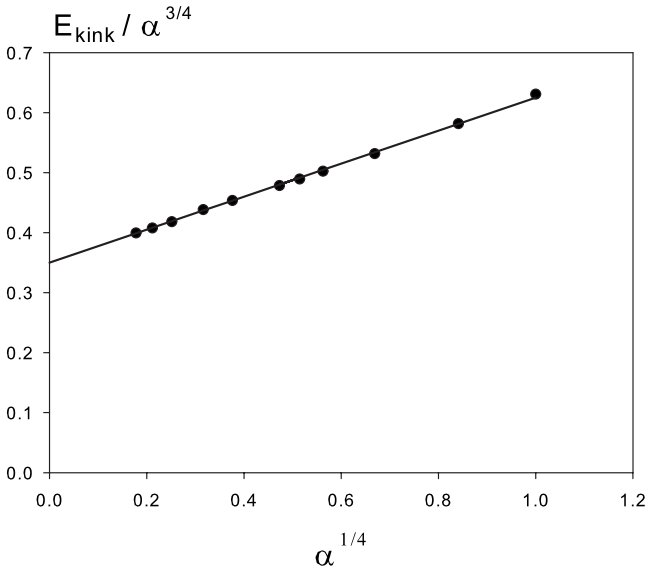

FIG. 3. The dependence $E_{\mathrm{kink}}/\alpha^{3/4}$ vs $\alpha^{1/4}$ for open chains at $\lambda=1/4$. Linear fit corresponds to $E_{\mathrm{kink}}=0.35\alpha^{3/4}+0.275\alpha$.

As one can see the correction term 0.275α gives substantial contribution for not too small α and cannot be neglected (for example, for $\alpha=0.1$ it gives near 30% of the kink energy). Therefore, one has to take it into account and rewrite Eq. (46) as

$$E_{\mathrm{kink}} = \alpha^{3/4} f_\mu(\mu) + \alpha g_\mu(\mu). \tag{51}$$

The linear terms in the expansion of functions $f_\mu(\mu)$ and $g_\mu(\mu)$ in μ correspond to the first order of PT (42) in $\frac{\gamma}{4}V_2$ and are defined by the behavior of the correlator $\langle \mathbf{S}_n \cdot \mathbf{S}_{n+2} - \frac{1}{4} \rangle$ at $\lambda=1/4$. The extrapolation of numerical calculations gives

$$\sum_n \left\langle \mathbf{S}_n \cdot \mathbf{S}_{n+2} - \frac{1}{4} \right\rangle \simeq 1.92\alpha^{1/4} - 0.84\alpha^{1/2}. \tag{52}$$

This means that for $|\mu| \ll 1$ the functions f_μ and g_μ are

$$f_\mu(\mu) \simeq 0.35 + 0.48\mu,$$

$$g_\mu(\mu) \simeq 0.275 - 0.21\mu. \tag{53}$$

It turns out that near the transition point it is sufficient to take the function $g_\mu(\mu)$ in a form of Eq. (53). This fact is confirmed by Fig. 4, where we present the dependence of $f_\mu(\mu)=[E_{\mathrm{kink}}-\alpha g_\mu(\mu)]/\alpha^{3/4}$ as a function of the scaling variable $\mu=\gamma/\sqrt{\alpha}$, calculated for different values of α and γ in the range $\alpha=0-1$ and $\gamma=-0.2-0.2$. All calculated points lie perfectly on one curve (see Fig. 4). This confirms the scaling form (51) in the vicinity of the transition point. As we see in Fig. 4 at $|\mu| \ll 1$ the function $f_\mu(\mu)$ has expansion (53). In the limit $\mu \gg 1$ the numerical calculations give $f_\mu(\mu) \simeq 0.65\sqrt{\mu}$.

To end this section we list the main results obtained by numerical calculations of finite chains for $\lambda \neq 0$. The m-magnon bound-state energy saturates for $m \gg 1$ for both rings and open chains, describing the finite gap in the spectrum. The multimagnon bound complexes with $m \gg 1$ are

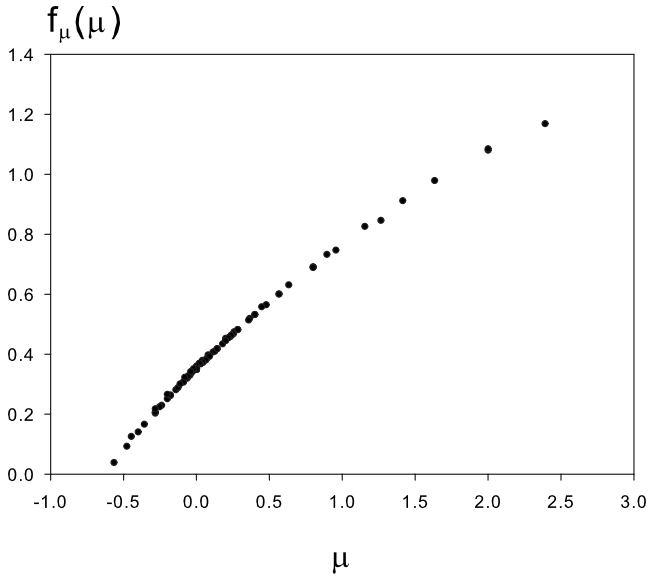

FIG. 4. The scaling function $f_\mu(\mu)$ in Eq. (46) for open chains. Circles correspond to different small values of γ and α. Circles form perfectly one curve, justifying the scaling dependence (46).

very massive, which results in flat band and quasidegeneracy of the bound m-magnon excitations for the rings over the total momentum k. This means that the total degeneracy of the "soliton" energy level E_s for the rings is proportional to N^2. In contrast to the rings, the m-magnon bound-state energy for the open chains is twofold degenerated for each m. Therefore, for the open chains the degeneracy of the kink energy level $E_{\rm kink}$ is proportional to N. The kink and soliton energies satisfy relation (49). These properties resemble those found for $\lambda=0$, though the energy of multimagnon excitations is modified for $\lambda\neq 0$. In particular, the critical exponent depends on λ.

It may be of interest to remark one point related to the bound magnon states in open chains. The lowest m-magnon state is the state with one domain wall (kink state) and it describes the gapped excitation above the fully polarized ground state. However, it is possible to realize this kink as the ground state. Let us add to Hamiltonian (2) the term with boundary magnetic fields,

$$-h(S_1^z - S_N^z). \tag{54}$$

Then there is a critical magnetic field h_c for which the kink energy is zero and the kink state is degenerate with the ferromagnetic state. It was shown in Ref. 28 that $h_c=\frac{1}{2}\sqrt{\Delta^2-1}$ for $\lambda=0$ and the critical field h_c does not depend on m. At $h=h_c$ the ground state is N-fold degenerate. It is a result of the special symmetry of Hamiltonian (2) for $\lambda=0$ with the boundary magnetic field $h=h_c$. This is not the case for $\lambda\neq 0$. In this case the magnetic field h_c depends on m. For example, $h_c(1)=\alpha^{3/4}/2^{1/4}\simeq 0.84\alpha^{3/4}$ for $\alpha\ll 1$ and $\lambda=1/4$. The value $h_c(m)$ decreases with m and saturates to $h_c\simeq 0.35\alpha^{3/4}$ for $m\gg 1$ and $\lambda=1/4$. For $h>h_c$ the kink state with $m=N/2(S^z=0)$ becomes the ground state.

VI. LOW-TEMPERATURE THERMODYNAMICS

Results of numerical calculations show that many peculiarities of the low-energy spectrum of model (2) at $\lambda\neq 0$ are similar to those for the anisotropic ferromagnetic chain. The thermodynamics of the latter model was studied in Ref. 29 and we use the arguments of this work to treat the low-temperature thermodynamics of model (2). As was shown in Ref. 29 the principal contributions to the partition function at low temperatures are given by two classes of the excited states: the spin waves and the multimagnon bound states. Both types of excitations are gapped and the existence of the gap implies an exponential behavior of the thermodynamic functions at $T\to 0$.

The leading terms for the free-energy at $T\to 0$ are given by a sum over low-lying states of both types. Certainly, the free energy must satisfy the natural condition to be proportional to N. This requires that the number of the excited states of each type must be proportional to N too. As for the spin waves the number of such states is $\sim N$ for both rings and open chains. But it is not the case for the multimagnon bound states. As was shown in Sec. V the number of these states for open chains is $\sim N$, while for rings it is $\sim N^2$. Therefore, as was already noticed in Sec. II, the correct contribution of the multi-magnon excitations to the free energy is given by those for the open chains (kinks) rather than for the rings (solitons),

$$F_{\rm bm}=-NT\exp\left(-\frac{E_{\rm kink}(\alpha,\lambda)}{T}\right), \tag{55}$$

where we set Boltzmann's constant $k_B=1$.

Of course, there is no difference between open chains and rings in the thermodynamic limit and Eq. (55) can be obtained using the rings as well. In this case a more complicated summation of high-lying excitations leads to the effective double reduction in the soliton energy E_s, which restores Eq. (55). For the case $\lambda=0$ this effect was studied in detail in Ref. 29.

The spin-wave contribution $F_{\rm sw}$ to the free energy is

$$F_{\rm sw}=-\frac{NT}{\pi}\int_0^\pi \exp\left(-\frac{E_1(k)}{T}\right)dk, \tag{56}$$

where $E_1(k)$ is one-magnon energy (10). The dominant contribution to the low-temperature free-energy is given by the excited states with the minimal value of the gap. Therefore, in order to identify the prevailing type of excitations we need to compare the kink energy $E_{\rm kink}$ with the spin-wave gap $E_{\rm sw}$, which corresponds to the minimum of one-magnon spectrum (10),

$$E_{\rm sw}=\alpha,\quad \lambda<\frac{1}{4},$$

$$E_{\rm sw}=\alpha-\frac{\gamma^2}{2},\quad \lambda\gtrsim\frac{1}{4}. \tag{57}$$

It turns out that there are two regions in the phase plane (λ,α) where the low-temperature thermodynamics is governed by different excitations (see Fig. 5). The boundary between these two regions $\alpha_c(\lambda)$ is determined by the equation

$$E_{\rm kink}(\alpha_c,\lambda)=E_{\rm sw}(\alpha_c,\lambda). \tag{58}$$

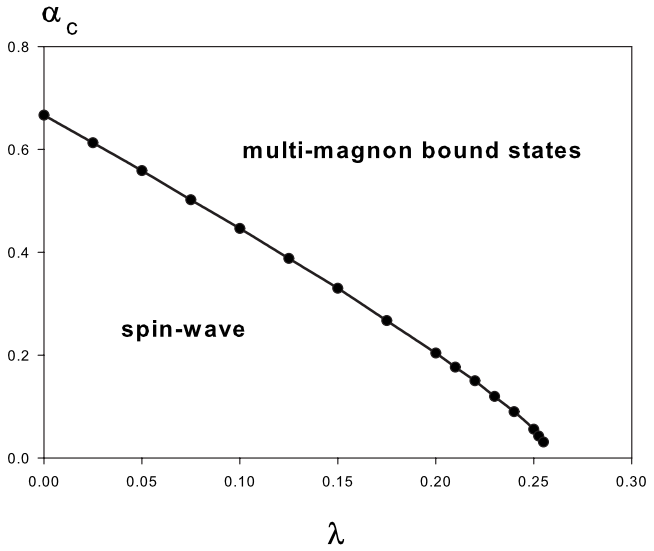

FIG. 5. The dependence $\alpha_c(\lambda)$. For $\alpha<\alpha_c$ the low-temperature thermodynamics is governed by spin-wave excitations, for $\alpha>\alpha_c$ by multimagnon bound states.

The calculated dependence $\alpha_c(\lambda)$ is shown in Fig. 5. In the region of the F phase below the curve $\alpha_c(\lambda)$ the dominant excitations are spin waves, while for $\alpha>\alpha_c(\lambda)$ they are multimagnon bound states. As follows from Fig. 5 the value $\alpha_c(\lambda)$ decreases when λ increases. In particular, $\alpha_c(0)=2/3$ and $\alpha_c(1/4)\simeq 0.046$.

The specific heat in the region with the spin-wave dominance is

$$C=\frac{\alpha^2 e^{-\alpha/T}}{T^{3/2}\sqrt{2\pi\gamma}},\quad \lambda<\frac{1}{4},\quad T\ll\gamma^2,$$

$$C=\frac{\alpha^2 e^{-\alpha/T}}{T^{7/4}2^{3/4}\Gamma(3/4)},\quad \lambda=\frac{1}{4},$$

$$C=\frac{\left(\alpha-\frac{1}{2}\gamma^2\right)^2 e^{\gamma^2/2T-\alpha/T}}{T^{3/2}\sqrt{\pi|\gamma|}},\quad \lambda\gtrsim\frac{1}{4},\quad T\ll\gamma^2. \tag{59}$$

In the region $\alpha>\alpha_c$ where the dominant contribution to the low-temperature thermodynamics is given by the multimagnon bound excitations the specific heat has an Ising-type behavior,

$$C=\frac{E_{\rm kink}^2}{T^2}\exp\left(-\frac{E_{\rm kink}}{T}\right). \tag{60}$$

To obtain the low-temperature susceptibility we add the magnetic field h along the Z axis. Then the spin-wave free energy $F_{\rm sw}$ has the same form as given by Eq. (56) with α replaced by $(\alpha+h)$ and the spin-wave contribution to the susceptibility is

$$\chi_{\rm sw}=-\frac{F_{\rm sw}}{T^2}. \tag{61}$$

In the presence of magnetic field the energy of m-magnon excitations is E_m+mh. The contribution to the low-temperature susceptibility of the multimagnon bound excitations can be obtained using the following arguments.[29] At $m\gg 1$ the magnons are tightly bound in the multimagnon complex and the size of the m-magnon bound state is m with the exponentially accuracy in m. Besides, these complexes are immobile because of their very large mass. Therefore, these bound states can be considered as domains of m neighbor overturned spins in the one-dimensional Ising model with the effective exchange constant $E_{\rm kink}(\alpha,\lambda)$. Using this analogy we obtain the multimagnon contribution to the zero-field susceptibility in the form

$$\chi_{\rm bm}=\frac{1}{4T}\exp\left(\frac{E_{\rm kink}}{T}\right). \tag{62}$$

Comparing Eqs. (61) and (62) one can easily see that the multimagnon contribution to the low-temperature susceptibility is dominant at all α and λ in contrast to the case of the specific heat.

We note that Eq. (62) determines the low-temperature susceptibility for the anisotropic model, i.e., for $\Delta>1$ and it is not valid in the limit $\Delta=1$, because the symmetry of the Hamiltonian changes at $\Delta=1$. For example, the susceptibility of the isotropic ferromagnetic Heisenberg chain ($\Delta=1,\lambda=0$) $\chi\sim 1/T^2$. The susceptibility for the isotropic F-AF model can be found using the modified spin-wave theory (MSWT).[36] We found that for $\lambda=1/4$ and $\Delta=1$ this method gives

$$\chi_{\rm MSWA}=\frac{1}{4(2T)^{4/3}}. \tag{63}$$

VII. DISCUSSION

Now, let us discuss a relevance of the considered model to the copper oxide Li_2CuO_2. This cuprate consists of the chains formed by the edge-sharing CuO_4 squares.[37] The magnetic interaction between NN spin-1/2 Cu^{2+} ions along the chain is ferromagnetic while an exchange interaction between NNN Cu ions is antiferromagnetic and these chains are described by the F-AF model. The magnetic structure of Li_2CuO_2 was determined by neutron-scattering experiments.[25] Below the Néel temperature $T_N\simeq 9$ K the spins of each CuO_2 chain have a ferromagnetic arrangement and the arrangement between neighboring chains is antiferromagnetic. At present the reason for the observed ferromagnetic in-chain order is unclear. The early estimations of the frustration parameter gave $\lambda\simeq 0.4-0.6$.[14,37] But for such values of the frustration parameter model (2) has a spiral-like ground state rather than the ferromagnetic one.[5,8] To resolve this discrepancy it was proposed that the observed ferromagnetic order arises due to the specific role of the interchain interactions.[37,38] However, recent estimations[26] of this value based on both exact diagonalization of Cu-O Hubbard model and the density-functional theory (DFT) calculations show that the frustration parameter is somewhat smaller than the critical value ($\lambda\simeq 0.23$). Therefore, we can suppose that in-

dividual noninteracting chains have the ferromagnetic ground state. The AF long-range order in Li_2CuO_2 below the Néel temperature arises due to a weak antiferromagnetic interchain interaction $J_\perp$.

A standard method for treating the quasi-one-dimensional systems is the mean-field approximation for the interchain interaction. In this approximation the Néel temperature is determined by the equation

$$zJ_\perp \chi_{1D}(T_N) = 1, \tag{64}$$

where χ_{1D} is the susceptibility of the individual chain and z is the transverse coordination number. In Li_2CuO_2 each CuO_2 chain is surrounded by four parallel neighboring chains and the only non-negligible coupling $J_\perp$ occurs between NNN spins on neighboring chains. Therefore, the effective coordination number is $z=8$.

To estimate T_N from Eq. (64) we use the susceptibility $\chi_{1D}(T)$ given by Eq. (62). According to Ref. 26 the frustration parameter for Li_2CuO_2 is close to the critical value and we take for the gap $E_{\rm kink}(\alpha,\lambda)$ its value at $\lambda=1/4$ and $\alpha \ll 1: E_{\rm kink}=|J_1|(0.35\alpha^{3/4}+0.275\alpha)$. The NN in-chain interaction J_1 and the interchain interaction $J_\perp$ were estimated in Refs. 26 and 39 as $J_1 \simeq -145$ K and $J_\perp \simeq 3.6$ K. Using these parameters we calculated the dependence $T_N(\alpha)$ shown in Fig. 6. According to these calculations the anisotropy corresponding to the Néel temperature of Li_2CuO_2 $T_N=9$ K is estimated as $\Delta \simeq 1.01$ (shown by the staggered lines in Fig. 6). Certainly, this estimate is based on the mean-field treatment which overestimates the transition temperature. Therefore, we expect that the anisotropy of the exchange interactions in Li_2CuO_2 is higher than our estimate 1% but does not exceed a few percent. The presence of anisotropy is also confirmed by the estimate of the Néel temperature for the isotropic case (see Fig. 6), where we used the MSWT susceptibility (63) in Eq. (64). The so obtained Néel temperature $T_N \simeq 7.5$ K is slightly lower than the experimental value $T_N \simeq 9$ K, confirming the presence of weak anisotropy. Though the anisotropy is very small it can essentially affect the excitation spectrum especially when the frustration parameter is close to the critical value $\lambda=1/4$.

In conclusion, we study the excitation spectrum of the one-dimensional anisotropic F-AF model in a parameter range corresponding to the ferromagnetic ground state. The remarkable feature of the spectrum is the existence of the multimagnon bound states. The lowest-lying m-magnon excitations are quasidegenerated and are separated by the gap from the ferromagnetic ground state. This gap as a function of α at $\alpha \ll 1$ has a power-law behavior with the exponent depending on the frustration parameter. It turns out that the gap for the bound multimagnon excitations in the rings is twice as large of that in the open chain. The multimagnon excitations together with the spin waves give dominant contributions to the low-temperature specific heat. The thermal gap characterizing the exponential behavior of the thermodynamic functions is the smallest value of two gaps: for one-magnon excitations and for bound multimagnon ones in *open chains*. The comparison of these gaps defines the regions of the dominance of one or another type of excitations. Contrary to the specific heat the zero-field susceptibility is always determined by the multimagnon excitations.

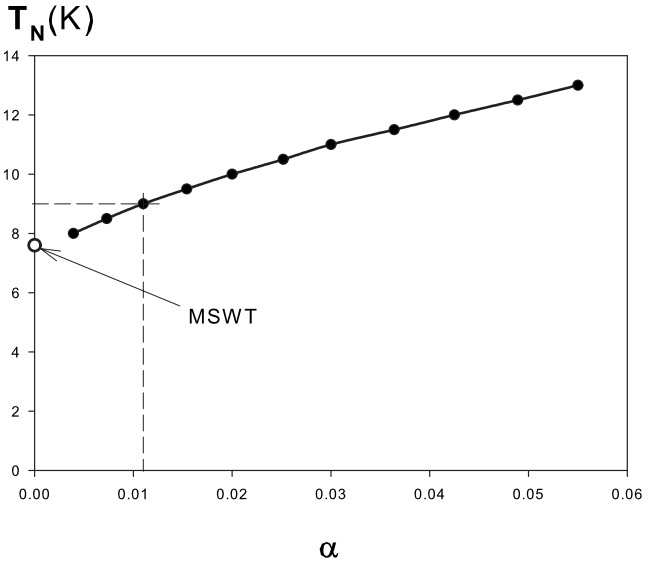

FIG. 6. The dependence of the Néel temperature T_N on α. Empty circle denotes the Néel temperature for the isotropic case calculated using the susceptibility MSWA (63). The staggered lines correspond to the estimate of the anisotropy in Li_2CuO_2.

ACKNOWLEDGMENTS

We would like to thank S.-L. Drechsler and D. Baeriswyl for valuable comments related to this work. D.V.D. thanks the University of Fribourg for kind hospitality. D.V.D. was supported by INTAS YS under Grant No. 05-109-4916. The numerical calculations were carried out with use of the ALPS Libraries.[40] This work was supported under RFBR Grant No. 09-02-90436.

*dmitriev@deom.chph.ras.ru

[1] H.-J. Mikeska and A. K. Kolezhuk, in *Quantum Magnetism*, Lecture Notes in Physics Vol. 645, edited by U. Schollwöck, J. Richter, D. J. J. Farnell, and R. F. Bishop (Springer-Verlag, Berlin, 2004), p. 1.

[2] F. D. M. Haldane, Phys. Rev. B **25**, 4925 (1982).

[3] T. Tonegawa and I. Harada, J. Phys. Soc. Jpn. **56**, 2153 (1987).

[4] K. Okamoto and K. Nomura, Phys. Lett. A **169**, 433 (1992).

[5] R. Bursill, G. A. Gehring, D. J. J. Farnell, J. B. Parkinson, T. Xiang, and C. Zeng, J. Phys.: Condens. Matter **7**, 8605 (1995).

[6] C. K. Majumdar and D. K. Ghosh, J. Math. Phys. **10**, 1388 (1969).

[7] S. R. White and I. Affleck, Phys. Rev. B **54**, 9862 (1996).

[8] T. Tonegawa and I. Harada, J. Phys. Soc. Jpn. **58**, 2902 (1989).

[9] A. V. Chubukov, Phys. Rev. B **44**, 4693 (1991).
[10] V. Ya. Krivnov and A. A. Ovchinnikov, Phys. Rev. B **53**, 6435 (1996).
[11] F. Heidrich-Meisner, A. Honecker, and T. Vekua, Phys. Rev. B **74**, 020403(R) (2006).
[12] H. T. Lu, Y. J. Wang, S. Qin, and T. Xiang, Phys. Rev. B **74**, 134425 (2006).
[13] A. A. Nersesyan, A. O. Gogolin, and F. H. L. Essler, Phys. Rev. Lett. **81**, 910 (1998).
[14] Y. Mizuno, T. Tohyama, S. Maekawa, T. Osafune, N. Motoyama, H. Eisaki, and S. Uchida, Phys. Rev. B **57**, 5326 (1998).
[15] M. Enderle, C. Mukherjee, B. Fak, R. K. Kremer, J.-M. Broto, H. Rosner, S.-L. Drechsler, J. Richter, J. Malek, A. Prokofiev, W. Assmus, S. Pujol, J.-L. Raggazzoni, H. Rakoto, M. Rheinstaedter, and H. M. Ronnow, Europhys. Lett. **70**, 237 (2005).
[16] S.-L. Drechsler, J. Richter, A. A. Gippius, A. Vasiliev, A. A. Bush, A. S. Moskvin, J. Malek, Y. Prots, W. Schnelle, and H. Rosner, Europhys. Lett. **73**, 83 (2006).
[17] M. Hase, H. Kuroe, K. Ozawa, O. Suzuki, H. Kitazawa, G. Kido, and T. Sekine, Phys. Rev. B **70**, 104426 (2004).
[18] S.-L. Drechsler, J. Richter, R. Kuzian, J. Malek, N. Tristan, B. Buechner, A. S. Moskvin, A. A. Gippius, A. Vasiliev, O. Volkova, A. Prokofiev, H. Rakoto, J.-M. Broto, W. Schnelle, M. Schmitt, A. Ormeci, C. Loison, and H. Rosner, J. Magn. Magn. Mater. **316**, 306 (2007).
[19] S.-L. Drechsler, N. Tristan, R. Klingeler, B. Büchner, J. Richter, J. Malek, O. Volkova, A. Vasiliev, M. Schmitt, A. Ormeci, C. Loison, W. Schnelle, and H. Rosner, J. Phys.: Condens. Matter **19**, 145230 (2007).
[20] D. V. Dmitriev and V. Ya. Krivnov, Phys. Rev. B **73**, 024402 (2006).
[21] D. C. Cabra, A. Honecker, and P. Pujol, Eur. Phys. J. B **13**, 55 (2000).
[22] C. Itoi and S. Qin, Phys. Rev. B **63**, 224423 (2001).
[23] H.-A. Krug von Nidda, L. E. Svistov, M. V. Eremin, R. M. Eremina, A. Loidl, V. Kataev, A. Validov, A. Prokofiev, and W. Assmus, Phys. Rev. B **65**, 134445 (2002).
[24] D. V. Dmitriev and V. Ya. Krivnov, Phys. Rev. B **77**, 024401 (2008).
[25] F. Sapina, J. Rodriguez-Carvajal, M. J. Sanchis, R. Ibanez, A. Beltran, and D. Beltran, Solid State Commun. **74**, 779 (1990).
[26] J. Malek, S.-L. Drechsler, U. Nitzsche, H. Rosner, and H. Eschrig, Phys. Rev. B **78**, 060508(R) (2008).
[27] A. A. Ovchinnikov, JETP Lett. **5**, 38 (1967).
[28] F. C. Alcaraz, S. R. Salinas, and W. F. Wreszinski, Phys. Rev. Lett. **75**, 930 (1995).
[29] J. D. Johnson and J. C. Bonner, Phys. Rev. B **22**, 251 (1980).
[30] R. O. Kuzian and S.-L. Drechsler, Phys. Rev. B **75**, 024401 (2007).
[31] A. A. Bahurmuz and P. D. Loly, J. Phys. C **19**, 2241 (1986).
[32] B. W. Southern, T. S. Liu, and D. A. Lavis, Phys. Rev. B **39**, 12160 (1989).
[33] L. Kecke, T. Momoi, and A. Furusaki, Phys. Rev. B **76**, 060407(R) (2007).
[34] D. C. Mattis, *The Theory Of Magnetism* (Harper and Row, New York, 1965), Sec. VI.
[35] D. V. Dmitriev, V. Ya. Krivnov, and J. Richter, Phys. Rev. B **75**, 014424 (2007).
[36] M. Takahashi, Phys. Rev. Lett. **58**, 168 (1987).
[37] Y. Mizuno, T. Tohyama, and S. Maekawa, Phys. Rev. B **60**, 6230 (1999).
[38] H. J. Xiang, C. Lee, and M.-H. Whangbo, Phys. Rev. B **76**, 220411(R) (2007).
[39] C. de Graaf, I. de P. R. Moreira, F. Illas, O. Iglesias, and A. Labarta, Phys. Rev. B **66**, 014448 (2002).
[40] F. Alet, P. Dayal, A. Grzesik, A. Honecker, M. Korner, A. Lauchli, S. R. Manmana, I. P. McCulloch, F. Michel, R. M. Noack, G. Schmid, U. Schollwock, F. Stockli, S. Todo, S. Trebst, M. Troyer, P. Werner, and S. Wessel, J. Phys. Soc. Jpn. **74**, 30 (2005).